

ENVIRONMENTAL FACTORS AFFECTING THE SPATIOTEMPORAL DISTRIBUTION OF *DECAPTERUS MARUADSI* IN THE WESTERN GUANGDONG WATERS, CHINA

YU, J.¹ – LIU, Z.-N.^{1,2} – CHEN, P.-M.¹ – YAO, L.-J.^{3*}

¹South China Sea Fisheries Research Institute, Chinese Academy of Fishery Sciences/Guangdong Provincial Key Laboratory of Fishery Ecology and Environment/Scientific Observing and Experimental Station of South China Sea Fishery Resources and Environment, Ministry of Agriculture and Rural Affairs/Guangdong Engineering Technology Research Center of Marine Recreational Fishery/Key Laboratory of Marine Ranching Technology, CAFS, Guangzhou 510300, China

²College of Marine Science, Shanghai Ocean University, Shanghai 201306, China

³Department of Optoelectronic Engineering, College of Science and Engineering, Jinan University, Guangzhou 510632, China

*Corresponding author
e-mail: constancecarson15@gmail.com

(Received 8th Mar 2019; accepted 21st May 2019)

Abstract. *Decapterus maruadsi* is a small pelagic fish and is of great significance to the ecosystems in the northern South China Sea. We collected and analyzed the data recorded by the fishing vessels in the western Guangdong waters in winter and summer and remote sensing data including sea surface temperature (SST), chlorophyll a concentration (Chl a) and sea level anomalies (SLA) from 2011 to 2015, using generalized additive model (GAM). Results showed that the catch per unit effort (CPUE) of *D. maruadsi* in the western Guangdong waters had a significant positive linear correlation with longitude, and the *D. maruadsi* populations were concentrated in the east of the study area. The total explanation of *D. maruadsi* CPUE in GAMs was 47.40%, among which, the factors year, month, lunar phase, latitude, Chl a, SLA and water depth explained 9.30%, 13.50%, 6.50%, 1.90%, 1.70%, 4.60%, and 9.90%, respectively. The *D. maruadsi* populations in the study were concentrated in the area of latitude 21°N, Chl a 0.1- 0.5 mg·m⁻³, SLA -0.05 m and water depth 80 m. Results of this work will help in understanding the environmental factors affecting *D. maruadsi* distribution in the western Guangdong waters.

Keywords: *generalized additive model, environmental factors, habitat suitability index (HSI), fisheries, main spawning habitats*

Introduction

Decapterus maruadsi, a pelagic fish in the family Carangidae (Perciformes), lives in warm waters, and is widely distributed along the coasts of Southeast China (Deng et al., 1991). It is one of the major species captured by pelagic trawls and light luring seine fishing vessels (Zheng et al., 2014; Thanh and Do, 2018). *D. maruadsi* has a short lifespan and fast growth and reproduction rate, and as an R-selected species, it is susceptible to fishing intensity and marine environment (Chen et al., 2003; Dai, 2017; Austin et al., 2018). The populations of *D. maruadsi* in the northern South China Sea shifted towards younger age and smaller size due to overfishing since the 1990s (Lu, 2000; Chen and Qiu, 2009). But the *D. maruadsi* resource is beginning to recover due to summer fishing moratorium and other fishery industry restructuring policies in recent years (Chen et al., 2010; Geng et al., 2018; Abija and Nwankwoala, 2018). As a small

pelagic fish, *D. maruadsi* has an important impact on the ecosystem output of the northern South China Sea (Chen and Qi, 2009). The sea area off western Guangdong is one of the main spawning habitats for *D. maruadsi* in the northern South China Sea (Chen et al., 2003), so it is of great significance to investigate the temporal and spatial distribution of this species in this area. At present, the existing studies on *D. maruadsi* are mostly focused on its biology (Jiang, 2012; Huang, 1995; Da, 2017), resource assessment (Chen and Qiu, 2003; Jamil et al., 2018), etc. Acoustic assessments indicate that carangid fish such as *D. maruadsi* along the east coast of Peninsular Malaysia are concentrated at 40-60 m below the ocean surface (Hashim, 2017; Tao, 2018). The studies that assessed the relationship between *D. maruadsi* fisheries and environmental factors in the northern South China Sea in different seasons based on the habitat suitability index (HSI) model indicated that chlorophyll a (Chl a) concentration is the determinant of the distribution of *D. maruadsi* fisheries in spring. In recent years, due to the increase in offshore fishing intensity, changes in ecological environment and climate, the resource stock and spatial distribution of many marine species have changed, which has a profound impact on fish habitats and ecosystems. Therefore, evaluating the correlation between *D. maruadsi* distribution and marine environmental factors in western Guangdong is important for the sustainable development of fisheries.

The relationship between fishery resources and marine environment is very complicated, as it is non-linear and non-additive (Stenseth et al., 2002, 2004; Dingstor et al., 2007; Tianlei, 2019), and the use of different observational scales can cause large differences in results (Fauchald et al., 2000). Therefore, it is crucial to choose a suitable method for quantitative analysis of the relationship between fishery resources and the marine environment. As the nonparametric extensions of generalized linear models (GLMs), generalized additive models (GAMs) provide flexible method for uncovering the nonlinear relationship between response and predictor variables (Hastie and Tibshirani, 1990; Jegatheesan and Zakaria, 2018), and thus are suitable for exploring the nonlinear relationship between fishery resources and marine environment (Stoner, 2001; Agenbag, 2003). GAMs not only can be used for different species or different seas, but also can be combined with a variety of environmental factors to better reveal the relationship between environmental factors and the variation, spatial distribution, temporal distribution of fishery resources (Venables et al., 2004; La et al., 2016; Bacha et al., 2017). The studies based on GAMs have shown that zooplankton biomass and the location of oceanic fronts have an impact on the distribution of *Clupea harengus* in the vicinity of the Shetland Islands (Maravelias et al., 1997). The spatial distribution of *Loligo spp.* and *Tachysurus* in the Arabian Sea was well predicted based on the data of sea surface temperature (SST), chlorophyll a (Chl a) concentration, photosynthetically active radiation (PRA) and sea level anomalies (SLA) in the study of Solanki (2017). The interaction between upwelling index, year and latitude had a great influence on the spatial distribution of sardines in Mauritanian waters (Bacha et al., 2017; Abdullah and Rahim, 2018). Wang et al. (2018) reported that prey density, water depth, bottom water temperature and distance to shore had a great influence on the distribution of Chinese white dolphin in western Pearl River Estuary.

In this study, generalized additive models (GAMs) were used to quantitatively analyze the main environmental factors affecting the spatiotemporal distribution of *D. maruadsi*, and to explore the formation mechanism of *D. maruadsi* fishery in the western Guangdong waters, and to provide a theoretical basis for fishery management and marine protected area planning under climate changes.

Materials and methods

Data collection

Fishery data

The data of *D. maruadsi* resource were from the observational records of large-scale light-luring seine fishing vessels in western Guangdong waters (19.75° to 21.75°N, 111.25°E to 113.75°E) in January, February, August and September from 2011 to 2015. The data (including working time, voyage, longitude, latitude and fish catch) were generated at a spatial resolution of 0.5° × 0.5° in latitude and longitude (one fishing area), and summarized by day (Fig. 1).

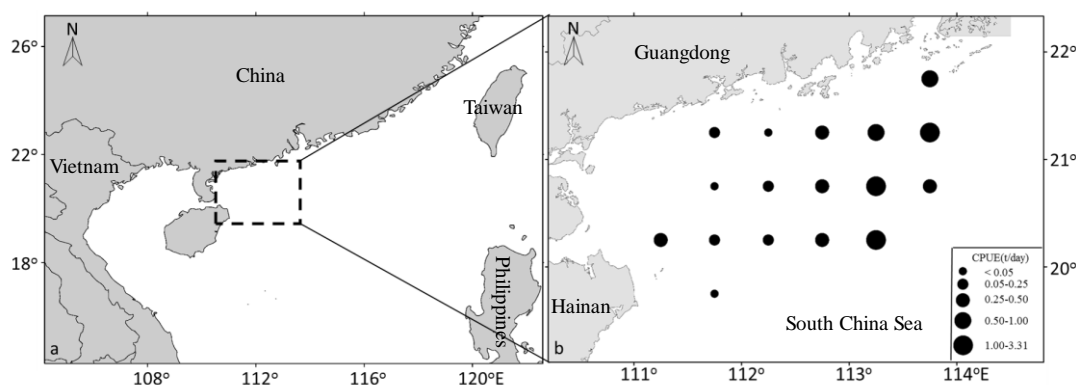


Figure 1. Distribution of *D. maruadsi* CPUE in western Guangdong waters

Environmental data

The remote sensing data including chlorophyll a concentration (Chl a), sea surface temperature (SST) and sea level anomalies (SLA) were used in this study. Among them, Chl a and SST were from MODIS Aqua Level 3 data products (<https://oceancolor.gsfc.nasa.gov>), with a temporal resolution of one day and a spatial resolution of 4 km. SLA data were from CTOH/LEGOS website (<https://www.aviso.altimetry.fr/en/home.html>) with a temporal resolution of one day and a spatial resolution of 0.25°. Water depth data were acquired from Google Earth, with a spatial resolution of 70 m (Jaimes, 2017).

Data processing

CPUE (catch per unit effort) calculation (Campbel, 2004)

$$CPUE = \frac{c}{f} \quad (\text{Eq.1})$$

where, CPUE is the average daily *D. maruadsi* catch by a vessel (unit: tons per day), *c* is daily *D. maruadsi* catch in a 0.5° × 0.5° fishing grid (unit: tons), *f* is the number of operations in a 0.5° × 0.5° fishing grid (days).

Remote sensing data fusion (Fu et al., 2009)

The remote sensing data (Chl, SST and SLA) of the study area were extracted and merged using the formula as follows:

$$Average_j = \frac{\sum_{i=1}^m Value(i)_j}{m} \quad (\text{Eq.2})$$

where, $Average_j$ is the mean value of fused environmental data (Chl, SST and SLA) in fishing grid j , j is a $0.5^\circ \times 0.5^\circ$ fishing grid, m is the number of pixels of environmental data (Chl, SST, SLA) in fishing grid j , $Value(i)$ is the value of a single pixel in fishing area j .

GAM analysis

Generalized additive models (GAM) focus on exploring data nonparametrically, compared to generalized linear models (Feng, 2007; Sudhakaran et al., 2018). In order to avoid excessive computation and over-fitting, the linear correlation between *D. maruadsi* CPUE and each predictor variable was measured according to Pearson correlation coefficient R before GAM was constructed (Li, 2007; Le, 2017). When $R > 0.5$, the predictor variable has a linear relationship with *D. maruadsi* CPUE, and should be removed from the model. The R mgcv package was used to fit the GAM (Wood, 2004, 2011). The general form of the model can be written as:

$$g(\mu) = \beta + f_1(x_1) + \dots + f_i(x_i) + \varepsilon \quad (\text{Eq.3})$$

where $g(\mu)$ is the link function, which is the logarithm of CPUE + 1; β is the intercept term; f is a smooth function, i is the number of predictor variables, ε is the error term. The GAM procedure uses smoothing splines $s(\cdot)$.

Diagnosis of GAM

The predictor variables influencing *D. maruadsi* CPUE that should be incorporated into the model were identified applying a stepwise GAM and according to Akaike Information Criterion (AIC) (Shih, 2014; Franco et al., 2018). Models were built by adding in new terms and seeing how much they improved the fit, and by dropping terms that did not degrade the fit significantly. The influence of the predictors was assessed via F -test and chi-square test (Quinn and Deriso, 1999). AIC was calculated as follows (Venables, 2004):

$$AIC = \theta + 2df\delta$$

where θ is the deviance, df is the effective degree of freedom, and δ is the variance.

Violin plot

A violin plot, similar to a box plot with a rotated kernel density plot on each side, simultaneously reflects the statistical features (maximum, minimum, median, and upper and lower quartiles) and distribution of a set of data (Hintze, 1998). The violin plot was made using the ggplot2 package in R software from *D. maruadsi* CPUE in winters

(January and February) and summers (August and September). Since the average CPUE differed greatly, the ordinate was scaled logarithmically. Then the violin plot was used to analyze the difference in *D. maruadsi* CPUE between winters and summers in western Guangdong waters (Cortez, 2016).

Results

Linear correlation analysis between D. maruadsi CPUE and the influencing factors

Pearson correlation analysis on *D. maruadsi* CPUE and the factors influencing it including year, month, lunar phase, longitude (Lon), latitude (Lat), SST, Chl a, SLA and water depth (Table 1) showed that seven of the factors (month, lunar phase, longitude, latitude, SST, Chl a, SLA and depth) were significantly correlated with *D. maruadsi* CPUE ($P < 0.05$), and the correlation coefficient between longitude and CPUE was greater than 0.5 ($R > 0.5$), indicating that longitude had a strong positive linear correlation with *D. maruadsi* CPUE. Therefore, longitude was removed from the GAM.

Table 1. Pearson correlation coefficient of *Decapterus maruadsi* CPUE and Impact factors

Factors	Cor	P-value
Year	-0.067	0.345
Month	0.292	2.514*10 ⁻⁵
Lunar phase	-0.146	0.038
Lon	0.535	2.678*10 ⁻¹⁶
Lat	0.205	0.003
SST	0.261	1.830*10 ⁻⁴
Chl a	-0.167	0.018
SLA	-0.178	0.012
Depth	-0.163	0.021

Analysis of longitudinal distribution of *D. maruadsi* CPUE (Fig. 2) revealed that the maximum values of *D. maruadsi* CPUE within longitude 115.25°E - 113.75°E were 0.56 t/d, 1.00 t/d, 1.00 t/d, 3.00 t/d, 30.20 t/d and 18.00 t/d, respectively. The upper quartile of *D. maruadsi* CPUE increased with longitude increasing from 112.25°E to 113.75°E. The median value and lower quartile of *D. maruadsi* CPUE also increased with longitude increasing from 111.75°E to 113.75°E. There were fewest data at 111.25°E and most data 113.25 °E. To sum up, *D. maruadsi* CPUE value showed a general decreasing trend from east to west in the study area, and the high CPUE values were concentrated within 113.25°E-113.75°E.

Environmental effects on D. maruadsi CPUE based on GAM analysis

The GAM was built by adding in the temporal, spatial and environmental factors stepwise and seeing how much they improved the fit. The temporal, spatial and environmental variables included in the model were year, month, lunar phase, latitude, Chl a, SLA and depth (Table 2). The GAM could explain 47.40% of the variability in *D. maruadsi* CPUE in total, and the residual degrees of freedom was 185.23.

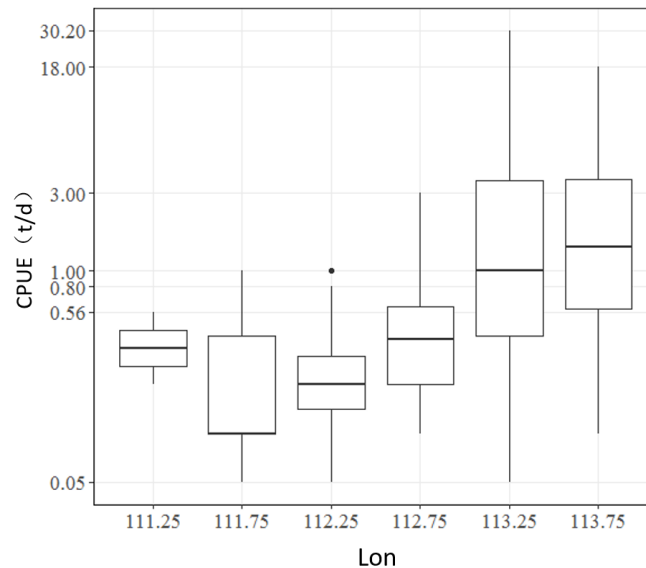


Figure 2. Box plot of longitudinal distribution of *D. maruadsi* CPUE

Table 2. Generalized additive models (GAMs) fitted to *D. maruadsi* CPUE and analysis of deviance

Factors	Residual degree of freedom	AIC value	Cumulative of deviance explained
$\text{Log}(\text{CPUE} + 1) = \text{NULL}$	200.00	16.34	0.00
$\text{Log}(\text{CPUE} + 1) = \text{s}(\text{Year})$	196.28	4.16	9.30%
$\text{Log}(\text{CPUE} + 1) = \text{s}(\text{Year}) + \text{s}(\text{Month})$	193.73	-23.09	22.80%
$\text{Log}(\text{CPUE} + 1) = \text{s}(\text{Year}) + \text{s}(\text{Month}) + \text{s}(\text{Lunar phase})$	191.87	-37.14	29.30%
$\text{Log}(\text{CPUE} + 1) = \text{s}(\text{Year}) + \text{s}(\text{Month}) + \text{s}(\text{Lunar phase}) + \text{s}(\text{Lat})$	191.08	-40.88	31.20%
$\text{Log}(\text{CPUE} + 1) = \text{s}(\text{Year}) + \text{s}(\text{Month}) + \text{s}(\text{Lunar phase}) + \text{s}(\text{Lat}) + \text{s}(\text{Chl a})$	190.24	-44.22	32.90%
$\text{Log}(\text{CPUE} + 1) = \text{s}(\text{Year}) + \text{s}(\text{Month}) + \text{s}(\text{Lunar phase}) + \text{s}(\text{Lat}) + \text{s}(\text{Chl a}) + \text{s}(\text{SLA})$	190.24	-54.73	37.50%
$\text{Log}(\text{CPUE} + 1) = \text{s}(\text{Year}) + \text{s}(\text{Month}) + \text{s}(\text{Lunar phase}) + \text{s}(\text{Lat}) + \text{s}(\text{Chl a}) + \text{s}(\text{SLA}) + \text{s}(\text{Depth})$	185.23	-83.23	47.40%
$\text{Log}(\text{CPUE} + 1) = \text{s}(\text{Year}) + \text{s}(\text{Month}) + \text{s}(\text{Lunar phase}) + \text{s}(\text{Lat}) + \text{s}(\text{Chl a}) + \text{s}(\text{SLA}) + \text{s}(\text{Depth}) + \text{s}(\text{SST})$	184.21	-82.33	47.70%

The contribution of each factor included in GAMs to *D. maruadsi* CPUE indicated their influence on *D. maruadsi* CPUE (Table 3). Among them, the most influential factor was month, which explained 13.50% of the variability in *D. maruadsi* CPUE, followed by depth, year, lunar phase, SLA, latitude, Chl a, which explained 9.9%, 9.30%, 6.50%, 4.60%, 1.90%, and 1.70% of the variability in *D. maruadsi* CPUE respectively. The *F* test and Chi-squared test showed that after SST was added into the model, it did not degrade the fit significantly ($P > 0.05$), while AIC value increased, suggesting that SST had no significant effect on *D. maruadsi* CPUE, so it was removed from the model.

Table 3. Statistical significance and contribution of the factors in GAM

Factors	Degree of freedom	P-value	F-test	Chi-square test	Contribution of selected variables
Year	3.69	1.35×10^{-3}	6.71×10^{-4}	4.51×10^{-4}	9.30%
Month	1.00	1.92×10^{-6}	6.02×10^{-7}	1.70×10^{-7}	13.50%
Lunar phase	1.91	2.80×10^{-4}	1.88×10^{-4}	1.27×10^{-4}	6.50%
Lat	1.72	1.30×10^{-2}	0.02	0.02	1.90%
Chl a	1.00	1.76×10^{-2}	0.03	0.03	1.70%
SLA	2.76	1.47×10^{-3}	5.47×10^{-4}	4.20×10^{-4}	4.60%
Depth	2.71	7.32×10^{-7}	1.61 6	4.31×10^{-7}	9.90%
SST	1.00	0.317	0.32	0.32	0.30%

Relationship between *D. maruadsi* CPUE and the influencing factors (Fig. 3). Among all temporal factors, the year factor showed a positive effect in 2011-2013 and 2014-2015 (Fig. 3a) and a negative effect in 2013-2014, with no significant change in the confidence interval (Fig. 3b). From January to February, and from August to September, *D. maruadsi* CPUE increased monotonously over time; the width of the confidence interval decreased between different seasons (from February to August), and increased within the same seasons (January to February, August to September). *D. maruadsi* CPUE monotonously decreased with lunar phase changing from 1 to 15, and monotonously increased with lunar phase changing from 15 to 30 (Fig. 3c), with no significant change in the confidence interval.

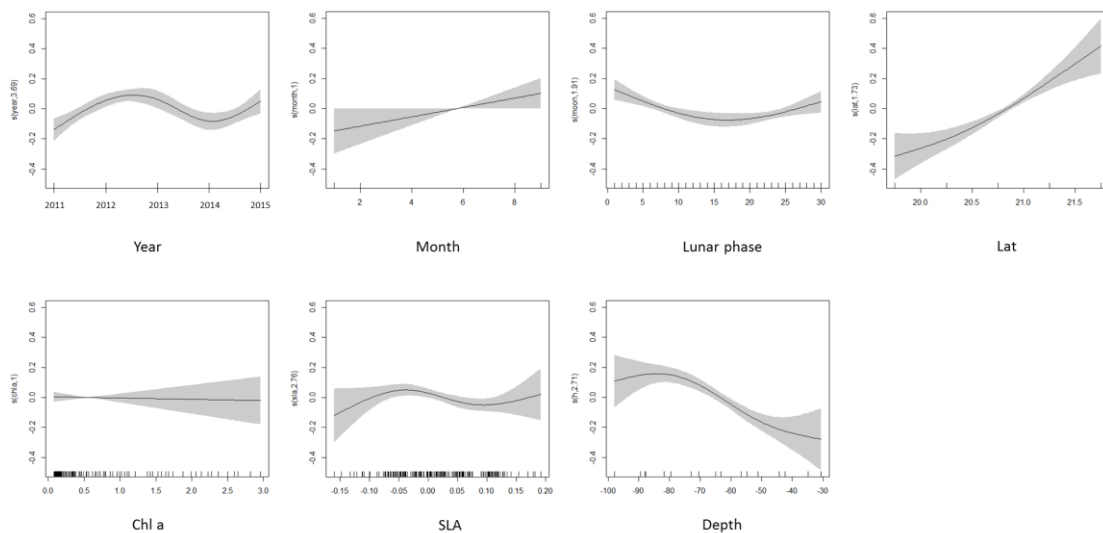


Figure 3. Effects of different factors on *D. CPUE* from GAM analysis. The shadow area indicates the 95% confidence intervals. Rug plots on the x-axis indicate data density

D. maruadsi CPUE increased monotonically with latitude increasing from 20°N to 21.5°N (Fig. 3d). The width of the confidence interval decreased within 20.5°N - 21.0°N, suggesting increased reliability of the estimation. The width of the confidence interval increased within 20.0°N -20.5°N and 21.0°N -21.5°N suggesting decreased reliability of the estimation.

D. maruadsi CPUE changed little with Chl *a* increasing (Fig. 3e). The data were concentrated within Chl *a* range of 0.1-0.5 mg·m⁻³, and the narrow confidence interval indicated high reliability of the estimation. With Chl *a* increasing in the range of 0.5-3.0 mg·m⁻³, the amount of data decreased, the width of confidence interval increased, indicating the reliability of the estimation decreased. It showed the effect of SLA on *D. maruadsi* CPUE (Fig. 3f). With SLA increasing from -0.15 to -0.05 m, *D. maruadsi* CPUE increased, and the width of confidence interval decreased. As SLA increased from -0.05 to 0.10 m, *D. maruadsi* CPUE decreased, the confidence interval became narrower, indicating the reliability of the estimation increased. As SLA increased from 0.10 to 0.20 m, *D. maruadsi* CPUE increased again, while the confidence interval became broader, and the reliability of the estimation decreased. The data were concentrated within SLA range of -0.8 to 0.13 m. It showed the effect of water depth on *D. maruadsi* CPUE (Fig. 3g). In detail, *D. maruadsi* CPUE increased with depth increasing from 30 to 80 m, while the width of confidence interval increased, indicating that the reliability of the estimation increased. With water depth increasing from 80 to 100 m, *D. maruadsi* CPUE declined, while the width of confidence interval increased, indicating that the reliability of the estimation reduced.

Seasonal variation in *D. maruadsi* CPUE

According to GAM analysis, the effect of the month factor which was most influential to *D. maruadsi* CPUE was further analyzed. The fishing vessels were operated in the sea area within 19.75°-21.75°N and 111.25°-113.75°E in January, February, August and September every year. Our data revealed that *D. maruadsi* CPUE was high in summer, with a maximum value of 18.00 t/d, a median value of 1.28 t/d, a minimum value of 0.00 t/d, and the abnormally high value in summer was 30.20 t/d. *D. maruadsi* CPUE was low in winter, with a maximum value of 1.25 t/d, a median of 0.20 t/d, and a minimum value of 0.00 t/d. Comparing the kernel density distribution plots of *D. maruadsi* CPUE between summer and winter, we found that the distribution of *D. maruadsi* CPUE in summer was discrete, with a peak value around 0.60, and that in winter was concentrated, with a peak value around 0.20. All the maximum value, upper quartile, median, and lower quartile of *D. maruadsi* CPUE in summer were higher than in winter (Fig. 4).

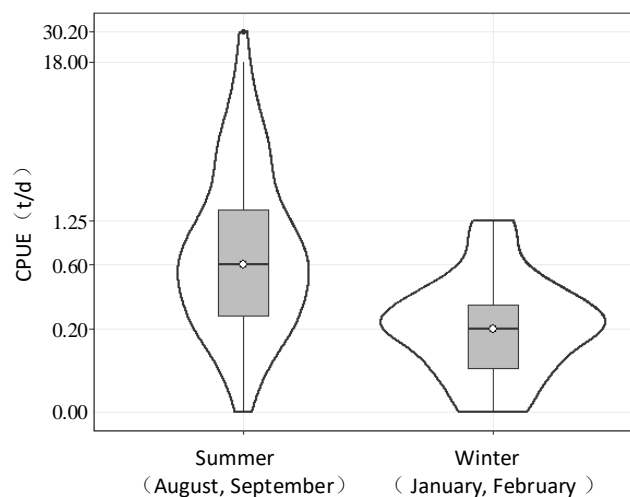


Figure 4. Violin plot of CPUE distribution of *Decapterus maruadsi* in summer and winter

Discussion

Relationship between D. maruadsi CPUE and temporal/spatial factors

GAMs analyze the relationship between response and predictor variables based on data model. They possess obvious advantages in analyzing the highly nonlinear and non-monotonic relationship between response and predictor variables, and can be used to reveal the unknown ecological relationships in fishery (Hastie et al., 1999; La et al., 2016; Bacha et al., 2017). Among all the factors included in GAM, the month factor made the greatest contribution to the GAM, up to 13.50% (Table 3). There was an obvious seasonal variation in *D. maruadsi* resources in western Guangdong waters, and its CPUE was higher in summer (August and September) than in winter (January and February) (Fig. 3b). Studies have shown that the spawning period of *D. maruadsi* begins at the end of winter and ends in summer (Chen et al., 2003; Wu, 2000). Previous studies on *D. maruadsi* in the Beibu Gulf and the Taiwan Strait indicates that summer is an important season for *D. maruadsi* to fatten up (Huang, 1995; Yang, 2016). *D. maruadsi* populations are able to increase during summer fishing moratorium (SFM) in June and July, and then gradually decrease from August to November due to the continuous high-intensity fishing in this period, resulting in significant difference in *D. maruadsi* CPUE between winter and summer.

The year factor explained 9.30% of the variability in *D. maruadsi* CPUE (Table 3). *D. maruadsi* CPUE fluctuated during 2011-2015 (Fig. 3a), and the decrease in 2014 was probably due to the unusually late summer monsoon season in the South China Sea in this year (Yuan, 2014). As an R-selected species, it is susceptible to environmental influence (Chen et al., 2003; Yan et al., 1987). The reduced fishing intensity during summer moratorium from June to July (Zhu, 2009; Qu, 2018), and the increased primary productivity caused by the upwelling in western Guangdong waters (Song, 2012) provide favorable conditions for the replenishment of *D. maruadsi* resources. It is widely accepted that summer winds may be the reason for the strong upwellings in the study area from June to July (Xie, 2016). The summer monsoon in the South China Sea in 2014 started unusually late, which might delay the occurrence of upwelling in this area, as a result, the *D. maruadsi* resources were not sufficiently replenished. In 2015, the summer monsoon in South China Sea occurred at the usual time (Si et al., 2016), and thus the *D. maruadsi* resources were able to recover during moratorium, so its CPUE in 2015 was higher than in 2014.

Lunar phase explained 6.50% of the deviance of the model (Table 3). The relationship between *D. maruadsi* CPUE and lunar phase was represented by an inverted U-shaped curve, with the minimum CPUE value at lunar phase 15 (Fig. 3c), which might be caused by the light luring seine used by the vessels. The moon is at its brightest when full in a month, and the moonlight lowers the attractiveness of light luring seines to cephalopods (Chen et al., 2006; Yan, 2015). As the major catch of light luring seine fishing in western Guangdong waters (Yang et al., 2009), similar results were obtained in *D. maruadsi* in our study. In addition to the influence of moonlight intensity, whether the changes in the marine environment caused by lunar phase have an impact on *D. maruadsi* CPUE needs to be further studied.

Correlation analysis indicated that there was a positive linear correlation between longitude and *D. maruadsi* CPUE in western Guangdong waters (Table 1). The violin plot (Fig. 2) showed that the maximum value, median value, and the amount of data of *D. maruadsi* CPUE were all higher at longitude 113.25°E-113.75°E. GAM analysis

showed that latitude and *D. maruadsi* CPUE had a high positive correlation near longitude 21°N (Fig. 3d). *D. maruadsi* tends to spawn in the areas where seawater is diluted by fresh water, and the spawning season lasts for a long period until the end of summer (Chen et al., 2003; Zhu, 1984). Therefore, *D. maruadsi* population tends to concentrate in the Pearl River estuary in winter and summer. The decreased water depth along coasts may be the factor restricting the positive effect of latitude, increasing the width of confidence interval north of 21°N, and reducing the reliability of the estimation.

Relationship between D. maruadsi CPUE and environmental factors

Among the environmental factors, water depth was the most influential to GAM, and it explained 9.90% of the deviance (Table 3). In detail, *D. maruadsi* CPUE increased monotonously with depth increasing from 30 to 80 m, and the reliability of the estimation was higher at depth 50-80 m. With further increase in water depth, *D. maruadsi* CPUE declined monotonously (Fig. 3g). *D. maruadsi* is a pelagic fish (Deng, 1991). Acoustic assessments indicate that three carangid species including *D. maruadsi* along the east coast of Peninsular Malaysia are concentrated at depth of 40-60 m, and their density is 0 when water depth exceeds 80 m. The depth of study area is about 0-200 m. While some researchers believe that *D. maruadsi* in this sea area lives at or near the bottom of the sea (Fan, 2018). The GAMs showed that in western Guangdong waters, the high CPUE values of *D. maruadsi* appeared at about 80 m, which might have been affected by light luring seines.

SLA explained 4.6% of the total deviance (Table 3). The positive effect of SLA on *D. maruadsi* CPUE peaked at SLA around -0.05 m (Fig. 3f), which may be related to oceanic currents (such as eddies, upwelling) in this area. Remote sensing data about sea surface height such as SLA and sea surface height anomaly (SSHA) are the indicators of oceanic currents and density stratification of seawater (Thomas, 2012), and are widely used for eddy identification (Wang, 2015; Yi, 2014; Zhan, 2014). Eddies regulates SST, SSS, and Chl a by a complicated mechanism (Chelton, 2011; Schütte, 2016; He, 2016). The center of anticyclonic eddies in the northeastern Atlantic is characterized by a negative SLA value and a reduced SST and SSS (Schütte, 2016). Along the coasts of the southwest Indian Ocean, the cold eddies have a negative SSHA value at their center, and stir up nutrients from the bottom, resulting in an elevation in Chl a. In the northern South China Sea, the positive effect of eddies on Chl a is stronger than the negative effect of anticyclonic eddies. And the eddies in the northern South China Sea increased seawater Chl a and promoted the transport of Chl a along longitude. In addition, SLA in upwelling region also exhibits a certain pattern. In West Africa, the upwelling center has a negative SLA, decreased SST and elevated Chl a (Nieto, 2017). The eastern Hainan-western Guangdong upwelling in the study area increased the Chl a and primary productivity in the area in summer (Song, 2012; He, 2016). Therefore, it is speculated that the oceanic currents (eddies, upwelling, etc.) at SLA -0.05 m provide favorable conditions for *D. maruadsi*, so that the positive effect of SLA on *D. maruadsi* CPUE reaches the maximum level within this SLA range.

No significant correlation between *D. maruadsi* CPUE and Chl a was observed in this study (Fig. 3e), but the data density plot indicated that *D. maruadsi* CPUE was concentrated at Chl a ranging from 0.1 to 0.5 mg·m⁻³, suggesting that *D. maruadsi* tends to live in waters with this range of Chl a. As an indicator of marine phytoplankton, Chl a has an important impact on fishery distribution. The study on the Pacific saury

(*Cololabis saira*) distribution in the northwestern Pacific Ocean based on empirical cumulative distribution function (ECDF) showed that high CPUE occurred when Chl a ranged from 0.4 to 0.6 mg·m⁻³ (Tseng, 2013). The study on yellowfin tuna (*Thunnus albacares*) in the western and central Pacific showed that the tuna tends to live in the waters with Chl a of 0.1-0.6 mg·m⁻³ (Wang, 2016; Kang, 2018). It has been reported that *D. maruadsi* in southern Taiwan Strait prefer to live in the waters with Chl a ranging from 0.2 to 1.0 mg·m⁻³ (Li, 2006). The data density distribution based on GAM analysis in this study revealed a Chl a range suitable for *D. maruadsi* in the western Guangdong waters.

Conclusions

To examine the relative influence of environmental factors on the distribution of *D. maruadsi*, data recorded by the fishing vessels and remote sensing including SST, Chl a and SLA in the western Guangdong waters, were analyzed using GAMs combined with correlation analysis in this study. Results showed that *D. maruadsi* CPUE in western Guangdong waters had a significant positive linear correlation with longitude, showing a general trend of decreasing from east to west. The final model explained 47.40% of the variability in *D. maruadsi* CPUE in total. Among all the factors included in the model, month was most influential to the distribution of *D. maruadsi*, followed by depth, year, lunar phase, SLA and latitude, Chl a and SST. The *D. maruadsi* resources were concentrated in the areas where the latitude was 21°N, Chl a ranged from 0.1 to 0.5 mg·m⁻³, SLA was -0.05 m and water depth was 80 m. The fishing method (light luring seines) used in this study might affect the conclusions about the effects of lunar phase and water depth on *D. maruadsi* CPUE. Therefore, different fishing methods will be used verify the effects of the two factors in the future work.

Acknowledgements. This study was supported by the following funds: (1) Central Public-interest Scientific Institution Basal Research Fund, CAFS (2018HY-ZD0104), (2) National Key R&D Program of China (2018YFD0900901); (3) Natural Science Foundation of Guangdong Province, China (2018A030313120), (4) State Key Laboratory of Tropical Oceanography, South China Sea Institute of Oceanology, Chinese Academy of Sciences (LTO1806).

REFERENCES

- [1] Abdullah, N. A., Rahim, F. (2018): Distinctiveness and potentials of two flowering roadside hedgerows, *Turnera ulmifolia* and *Melastoma malabathricum* as beneficial plants for insects. – *Environment & Ecosystem Science* 2(2): 06-10.
- [2] Abija, F. A., Nwankwoala, H. O. (2018): Characterization of aquifers in parts of Abia State Southeastern Nigeria. – *Earth Sciences Pakistan* 2(1): 18-22.
- [3] Agenbag, J. J., Richardson, A. J., Demarcq, H. et al. (2003): Estimating environmental preferences of South African pelagic fish species using catch size- and remote sensing data. – *Progress in Oceanography* 59(2): 275-300.
- [4] Austin, O. E., Ebuka, A. O., Zanders, A. C. C., Joseph, I. N. (2018): Seismic analysis of the transgressive systems tracts (TSTS) of the Niger Delta. – *Earth Sciences Malaysia* 2(2): 16-19.
- [5] Bacha, M, Jeyid. M. A., Vantrepotte, V. et al. (2017): Environmental effects on the spatio-temporal patterns of abundance and distribution of *Sardina pilchardus* and

- sardinella off the Mauritanian coast (North-West Africa). – Fisheries Oceanography 8(5): 12-25.
- [6] Campbell, R. A. (2004): CPUE standardisation and the construction of indices of stock abundance in a spatially varying fishery using general linear models. – Fisheries Research (Amsterdam) 70(2-3): 0-227.
- [7] Chelton, D. B., Samelson, R. M. (2011): The influence of nonlinear mesoscale eddies on near-surface oceanic chlorophyll. – Science 334(6054): 328.
- [8] Chen, G. B., Qiu, Y. S. (2003): Study on growth, mortality and reasonable utilization of *Decapterus maruadsi* in northern continental shelf waters of South China Sea. – Journal of Applied of Oceanography 22(4): 457-464.
- [9] Chen, G. B., Li, Y. Z., Chen, P. M. A. (2003): study on spawning ground of blue mackerel scad (*decapterus maruadsi*) in continental shelf waters of Northern South China Sea. – Journal of Tropical Oceanography 22(6): 22-28.
- [10] Chen, X. J., Tian, S. Q., Qian, W. G. (2006): Effect of moon phase on the jigging rate of *Ommastrephes bartrami* in the North Pacific. – Marine Fisheries 28(2): 136-140.
- [11] Chen, Z. Z., Qiu, Y. S. (2009): Assessment of the food-web structure, energy flows, and system attribute of northern South China Sea ecosystem. – Acta Ecologica Sinica 30(18): 4855-4865.
- [12] Chen, Z. Z., Lin, Z. J., Qiu, Y. S. (2010): Evaluation of sustainability of fisheries resources for South China Sea based on the AHP. – Journal of Natural Resources 25(2): 249-257.
- [13] Cortez, A. (2016): 3. Variabilidad espacio temporal de la precipitación en el estado Guárico, Venezuela. – Revista de la Facultad de Agronomía de la Universidad del Zulia 33(3).
- [14] Dai, J. G., Chen, Z. Z., Hunag, Z. R., Xu, Y. W., Sun, M. S., Zhang, K., Jiang, Y. E. (2017): Otolith morphology of *Decapterus maruadsi* in the continental shelf of northern South China Sea. – Journal of Applied of Oceanography 36(3): 417-426.
- [15] Deng, J. Y. (1991): Marine Biology. – China Agriculture Press, Beijing.
- [16] Dingstor, G. E., Ciannelli, L., Chan, K. S. et al. (2007): Density dependence and density independence during the early life stages of four marine fish stocks. – Ecology 88(3): 625-634.
- [17] Fan, J. T., Huang, Z. R., Xu, Y. W., Sun, M. S., Chen, G. B., Chen, Z. Z. (2018): Habitat model analysis for *decapterus maruadsi* in northern South China Sea based on remote sensing data. – Transactions of Oceanology and Limnology 3: 142-147.
- [18] Fauchald, P., Skarsfjord, H., Erikstad, K. E. (2000): Scale-dependent predator-prey interactions: the hierarchical spatial distribution of seabirds and prey. – Ecology 81(3): 773-783.
- [19] Franco, G. H., Macancela, N. A., Gavín-Quinchuela, T., Carrión-Mero, P. (2018): Participatory socio-ecological system: Manglaralto-Santa Elena, Ecuador. – Geology, Ecology, and Landscapes 2(4): 303-310.
- [20] Fu, D. Y., Pan, D. L., Ding, Y. Z., Zou, J. H. (2009): Quantitative study of effects of the sea chlorophyll-a concentration by typhoon based on remote-sensing. – Acta Oceanologica Sinica 31(3): 46-56.
- [21] Geng, P., Zhang, K., Chen, Z. Z. Xu, Y. W., Sun, M. S. (2018): Interannual change in biological traits and exploitation rate of *Decapterus maruadsi* in Beibu Gulf. – South China Fisheries Science 14(6): 1-9.
- [22] Hashim, M., Aziz, M. F. H. A., Hassan, R. B. et al. (2017): Assessing target strength, abundance, and biomass for three commercial pelagic fish species along the east coast of peninsular Malaysia using a split-beam echo sounder. – Journal of Coastal Research 33(6).
- [23] Hastie, T. J., Tibshirani, R. J. (1990): Generalized Additive Models. – Chapman and Hall, London, pp. 236-351.

- [24] He, Q., Zhan, H., Cai, S. et al. (2016): Eddy effects on surface chlorophyll in the northern South China Sea: mechanism investigation and temporal variability analysis. – Deep Sea Research Part I: Oceanographic Research Papers S0967063715301230.
- [25] Hintze, J., Nelson, R. (1998): Violin plots: a box plot-density trace synergism. – The American Statistician 52(2): 4.
- [26] Huang, M. Z. (1995): Feeding habits of *Decapterus maruadsi* in Taiwan Strait. – Journal of Applied of Oceanography (4): 399-406.
- [27] Jaimes, E. J. (2017): 2. Capacidad de carga y presión de uso de la tierra en cuatro sectores de la sub-cuenca del río Déleg, Provincia del Cañar, Ecuador. – Revista de la Facultad de Agronomía de la Universidad del Zulia 34(3).
- [28] Jamil, F., Arshad, R., Ali, M. A. (2018): Design, fabrication and evaluation of rotary hot-air dryer for the value addition of fruit waste. – Earth Sciences Pakistan 2(2): 07-11.
- [29] Jegatheesan, J., Zakaria, Z. (2018): Stress analysis on pressure vessel. – Environment & Ecosystem Science 2(2): 53-57.
- [30] Jiang, R. J., Xu, H. X., Jin, H. W., Zhou, Y. D., He, Z. T. (2012): Feeding habits of blue mackerel scad *Decapterus maruadsi* Temminck et Schlegel in the East China Sea. – Journal of Fisheries of China 36(2): 216-227.
- [31] Kang, L., Du, H. L., Zhang, H., Ma, W. L. (2018): Systematic research on the application of steel slag resources under the background of big data. – Complexity. doi.org/10.1155/2018/6703908.
- [32] La Mesa, M., La Mesa, G., Catalano, B. et al. (2016): Spatial distribution pattern and physical-biological interactions in the larval notothenioid fish assemblages from the Bransfield Strait and adjacent waters. – Fisheries Oceanography 25(6): 624-636.
- [33] Le, K., Yao, J. Z., Li, Z., Ke, Z. (2017): Preparation, characterization and photocatalytic activity of novel CeO₂ loaded porous alkali-activated steel slag-based binding material. – International Journal of Hydrogen Energy 42(27): 17341-17349.
- [34] Li, X. D. (2006): Monthly variability in the catchability of chub mackerel and round scad and its relationship with environmental seasonality in the southern Taiwan Strait. – Xiamen University, Xiamen, pp. 40-72.
- [35] Lu, Z. B., Dai, Q. S. (2000): An estimation of resources of chub mackerel, round scad and other pelagic fish stocks in the Taiwan Strait and the adjacent waters. – Journal of Fishery Sciences of China 7(1): 41-45.
- [36] Maravelias, C. D., Reid, D. G. (1997): Identifying the effects of oceanographic features and zooplankton on prespawning herring abundance using generalized additive models. – Marine Ecology Progress 147(1-3): 1-9.
- [37] Nieto, K., Mélin, F. (2017): Variability of chlorophyll-a concentration in the Gulf of Guinea and its relation to physical oceanographic variables. – Progress in Oceanography 151: 97-115.
- [38] Qu, Y. N., Pei, Z. B., Yang, S. T. (2018): Legal consideration on China's summer marine fishing moratorium system: in the perspective of venables sustainable development. – Ocean Development and Management 9.
- [39] Quinn, T. J., Deriso, R. B. (1999): Quantitative Fish Dynamic. – Oxford University Press, New York, pp. 124-256.
- [40] Schütte, F., Brandt, P., Karstensen, J. (2016): Occurrence and characteristics of mesoscale eddies in the tropical northeast Atlantic Ocean. – Ocean Science 12(3): 663-685.
- [41] Shih, C., Chen, Y., Hsu, C. (2014): Modeling the effect of environmental factors on the ricker stock-recruitment relationship for north pacific albacore using generalized additive models. – Terrestrial Atmospheric & Oceanic Sciences 25: 581-590.
- [42] Si, D., Liu, Y. J., Shao, X., Wang, Y. J. (2016): Anomalies of oceanic and atmospheric circulation in 2015 and their impacts on climate in China. – Meteorological Monthly 42(4): 481-488.

- [43] Solanki, H. U., Bhatpuria, D., Chauhan, P. (2017): Applications of generalized additive model (GAM) to satellite-derived variables and fishery data for prediction of fishery resources distributions in the Arabian Sea. – *Geocarto International* 32(1): 14.
- [44] Song, X., Lai, Z., Ji, R., Chen, C., Zhang, J., Huang, L., Yin, J., Wang, Y., Lian, S. Zhu, X. (2012): Summertime primary production in northwest South China Sea: interaction of coastal eddy, upwelling and biological processes. – *Continental Shelf Research* 48(5): 110-121.
- [45] Stenseth, N. C., Mysterud, A., Ottersen, G. et al. (2002): Ecological effects of climate fluctuations. – *Science* 297(5585): 1292-1296.
- [46] Stoner, A. W., Manderson, J. P., Pessutti, J. P. (2001): Spatially explicit analysis of estuarine habitat for juvenile winter flounder: combining generalized additive models and geographic information systems. – *Marine Ecology Progress* 213(4): 253-271.
- [47] Sudhakaran, M., Ramamoorthy, D., Savitha, V., Balamurugan, S. (2018): Assessment of trace elements and its influence on physico-chemical and biological properties in coastal agroecosystem soil, Puducherry region. – *Geology, Ecology, and Landscapes* 2(3): 169-176.
- [48] Tao, S. (2018): Evaluation of technology innovation in Hubei Province. – *Engineering Heritage Journal* 2(2): 09-10.
- [49] Thanh, L. D., Do, P. V. (2018): Streaming current induced by fluid flow in porous media. – *Earth Sciences Malaysia* 2(1): 22-28.
- [50] Thomas, A. C., Strub, P. T., Weatherbee, R. A. et al. (2012): Satellite views of Pacific chlorophyll variability: comparisons to physical variability, local versus nonlocal influences and links to climate indices. – *Deep Sea Research Part II Topical Studies in Oceanography* 77-80(10): 99-116.
- [51] Tianlei, W. (2019): Nonlinear control strategies and planning for underactuated overhead cranes. – *Engineering Heritage Journal* 3(1): 09-12.
- [52] Tseng, C. T., Su, N. J., Sun, C. L. et al. (2013): Spatial and temporal variability of the Pacific saury (*Cololabis saira*) distribution in the northwestern Pacific Ocean. – *Ices Journal of Marine Science* 70(5): 991-999.
- [53] Venables, W. N., Dichmont, C. M. (2004): GLMs, GAMs and GLMMs: an overview of theory for applications in fisheries research. – *Fisheries Research* 70(2-3): 315-333.
- [54] Wang, J., Chen, X., Chen, Y. (2016): Spatio-temporal distribution of skipjack in relation to oceanographic conditions in the west-central Pacific Ocean. – *International Journal of Remote Sensing* 37(24): 6149-6164.
- [55] Wang, X. X., Chen, T., Li, M., Wang, X. H., Wang, Y. Z. (2018): Relationships between environmental factors and the distribution of Indo-Pacific humpback dolphins (*Sousa chinensis*) in the western Pearl River Estuary, China. – *Acta Ecologica Sinica* 38(03): 934-944.
- [56] Wang, Z., Li, Q., Sun, L. et al. (2015): The most typical shape of oceanic mesoscale eddies from global satellite sea level observations. – *Frontiers of Earth Science* 9(2): 202-208.
- [57] Wood, S. N. (2004): Stable and efficient multiple smoothing parameter estimation for generalized additive models. – *J. Amer. Statist. Ass.* 99: 673-686.
- [58] Wood, S. N. (2011): Fast stable restricted maximum likelihood and marginal likelihood estimation of semiparametric generalized linear models. – *Journal of the Royal Statistical Society (B)* 73(1): 3-36.
- [59] Wu, Z. Q., Qiu, S. Y., Yang, S. Y. (2000): Characters of reproductive biology of six pelagic fishes in Minnan-Taiwan bank fishing ground. – *Marine Science Bulletin* 19(2): 25-29.
- [60] Xie, L. L., Zong, X. L., Yin, X. F., Li, M. (2016): The interannual variation and long-term trend of Qiongdong Upwelling. – *Oceanologia et Limnologia Sinica* 47(1): 43-51.

- [61] Yan, L., Zhang, P., Yang, L., Yang, B. Z., Chen, S., Li, Y. N., Tan, Y. G. (2015): Effect of moon phase on fishing rate by light falling-net fishing vessels of *Symplectoteuthis oualaniensis* in the South China Sea. – South China Fisheries Science 3: 16-21.
- [62] Yan, Y. M., Lu, Z. B., Dai, Q. S. (1987): Study on growth characteristics of round scad in Minzhong and Mindong fishing grounds. – Journal of Zoology 22(5): 8-13.
- [63] Yang, L., Zhang, X. F., Tan, Y. G., Zhang, P. (2009): The catch composition of light falling-net fishing and its impact on fishery resources in the northern South China Sea. – South China Fisheries Science 5(4): 41-46.
- [64] Yang, L., Cao, W. Q., Lin, Y. S., Chen, Y. H., Lin, Z. J., Wang, X. H. (2016): Preliminary study on feeding habits and trophic niche of nine economic fish species in Beibu Gulf in summer. – Journal of Tropical Oceanography 35(2): 66-75.
- [65] Yi, J., Du, Y., He, Z. et al. (2014): Enhancing the accuracy of automatic eddy detection and the capability of recognizing the multi-core structures from maps of sea level anomaly. – Ocean Science 10(1): 39-48.
- [66] Yuan, Y., Liu, Y. J., Wang, Y. J., Wang, P. L. (2014): Main characteristics and possible causes for the climate in China during the spring of 2014. – Meteorological Monthly 41(10): 1292-1297.
- [67] Zhan, P., Subramanian, A. C., Yao, F. et al. (2014): Eddies in the Red Sea: a statistical and dynamical study. – Journal of Geophysical Research Oceans 119(6): 3909-3925.
- [68] Zheng, Y. J., Li, J. S., Zhang, Q. Y., Hong, W. S. (2014): Research progresses of resource biology of important marine pelagic food fishes in China. – Journal of Fisheries of China 38(1): 149-160.
- [69] Zhu, D. L., Song, H. T., Bo, Z. L., Wu, Z. J. (1984): A study on mackerel and round scadfishing ground off Zhejiang coast in the summer-autumn season. – Marine Science Bulletin 3(2): 64-72.
- [70] Zhu, Y. G. (2009): Research on the Effects of China's Summer Fishing Moratorium - A Perspective of Institutional Analysis. – Ocean University of China, Qingdao, pp. 89-95.